LWT - Food Science and Technology 57 (2014) 106–115

Contents lists available at ScienceDirect

LWT - Food Science and Technology

journal homepage: www.elsevier.com/locate/lwt

Thermo-compression of biodegradable thermoplastic corn starch films containing chitin and chitosan

O. Lopez [a,b,*], M.A. Garcia [b], M.A. Villar [a], A. Gentili [d], M.S. Rodriguez [c], L. Albertengo [c]

[a] Planta Piloto de Ingeniería Química, PLAPIQUI (UNS-CONICET), Departamento de Ingeniería Química, UNS, Camino La Carrindanga km. 7, 8000 Bahía Blanca, Argentina
[b] Centro de Investigación y Desarrollo en Criotecnología de Alimentos, CIDCA (UNLP-CONICET), Facultad de Ciencias Exactas, UNLP, 47 y 116, 1900 La Plata, Argentina
[c] Instituto de Química del Sur, INQUISUR (UNS–CONICET), Laboratorio de Investigaciones Básicas y Aplicadas en Quitina, LIBAQ-Departamento de Química, UNS, Bahía Blanca, Argentina
[d] Departamento de Biología, Bioquímica y Farmacia, UNS, Bahía Blanca, Argentina

ARTICLE INFO

Article history:
Received 2 August 2013
Received in revised form
3 January 2014
Accepted 17 January 2014

Keywords:
Thermoplastic corn starch films with chitosan and chitin
Thermo-compression
Structural characterization
Barrier and mechanical properties
Antimicrobial capacity

ABSTRACT

Films based on thermoplastic corn starch (TPS) and chitosan/chitin were obtained by melt-mixing and thermo-compression. Chitosan and chitin incorporation to TPS matrix induced some structural modifications due mainly to the interactions between starch hydroxyl and chitosan/chitin amino groups. Crystallinity degree of TPS films was increased with biopolymers incorporation. Enthalpy melting values for TPS–chitosan/chitin films resulted lower than those corresponding to TPS control ones. Films had homogeneous and smooth surfaces, without pores and cracks and no glycerol migration was evidenced by Scanning Electronic Microscopy. Films fracture surfaces were uniform without the presence of unmelting starch granules neither chitosan/chitin agglomerates. Films with chitosan/chitin presented higher color, UV absorption capacity and opacity than TPS films. Addition of 10 g chitosan or chitin/100 g starch decreased 35 and 56% water vapor permeability, respectively. Biopolymers addition to TPS increased tensile strength and elastic modulus, and decreased elongation at break. Starch and glycerol-rich domains where evidenced in TPS matrixes by Dynamic Mechanical Analysis. Finally, TPS–chitosan films reduced *Staphylococcus aureus* and *Escherichia coli* growth in the contact zone.

1. Introduction

Packaging films, made of synthetic polymers, cause serious ecological problems due to their non-biodegradability. The major concern of consumers for environmental protection led packaging industries to increase research in biodegradable packaging materials (Fajardo et al., 2010). Materials based on polysaccharides are mostly ecological because they can degrade without leaving behind ecologically harmful residues, in contrast to those which are made from synthetic polymers (Simkovic, 2013). In this sense, polysaccharides are considered good candidates for biodegradable films since they are widely distributed in nature and have been regarded as structural materials. Among them, starch has been broadly used due to its abundance, low cost, and renewability (Xu, Kimb, Hanna, & Nag, 2005), being corn the major commercial starch source in the world (Mali, Karam, Pereira Ramos, & Grossmann, 2004). Unfortunately, starch films are sensitive to environmental humidity and brittle, as well as, difficult to process. Thus, their technological applications require the improvement of films mechanical and barrier properties. In order to overcome this limitation, corn starch has been blended with several synthetic and natural polymers. For example, wheat starch multilayer films with different aliphatic polyesters (Martin, Schwach, Avérous, & Couturier, 2001), films based on thermoplastic starch/natural rubber blends (Carvalho, Job, Alves, Curvelo, & Gandini, 2003) and blown-extrusion starch–pectin films (Fishman, Coffin, Konstance, & Onwulata, 2000), have being developed among others. An alternative, largely used to improve starch films properties, is the addition of chitosan to formulations, mainly due to the more hydrophobic character of chitosan compared to starch (Chillo et al., 2008; Fajardo et al., 2010; Lazaridou & Biliaderis, 2002; Pelissari, Yamashita, & Grossmann, 2011; Pelissari et al., 2012; Quattara, Simard, Piette, Begin, & Holley, 2000).

Chitosan is a partially deacetylated form of chitin, which is the most abundant natural polymer after cellulose (Rinaudo, 2006).

* Corresponding author. Planta Piloto de Ingeniería Química, PLAPIQUI (UNS-CONICET), Departamento de Ingeniería Química, UNS, Camino La Carrindanga km. 7, 8000 Bahía Blanca, Argentina.
E-mail address: ovlopez75@yahoo.com.ar (O. Lopez).

0023-6438/$ – see front matter © 2014 Elsevier Ltd. All rights reserved.
http://dx.doi.org/10.1016/j.lwt.2014.01.024

Chitin is found in the skeletal materials of crustaceans, insects and cell walls of bacteria and fungi. Although in the literature are several studies related to starch-based films with chitosan, chitin use has not been reported. Chitosan is nontoxic, biodegradable, compatible with other biopolymers and is used to functionalize many others polysaccharides (Zhai, Zhao, Yoshii, & Kume, 2004). Moreover, the antibacterial and antifungal properties of chitosan have been studied by several authors; molecular weight and amino groups are the responsible of chitosan antibacterial capacity (Le et al., 2001; Liu, Huan, Yang, Li, & Yao, 2001; Zhai et al., 2004).

Most of the works found in the literature related to starch-chitosan materials based their studies on films obtained by casting method. However, processing methods such as blown extrusion, compression or injection molding are less reported. Solvent-casting has been the most used method at small-scale of biopolymers films preparation, which involves solubilization, casting, and drying steps. Despite, this is a good and adequate technique at laboratory scale, it is considered as a high energy-consuming procedure. On the other hand, high levels and efficient biodegradable films production is required by industrial area. In this sense, scaling-up processing methods using equipments designed for synthetic polymers is indispensable (Sothornvit, Olsen, McHugh, & Krochta, 2007; Thunwall, Kuthanova, Boldizar, & Rigdahl, 2008). In this context, extrusion, blowing, injection, and thermo-compression are viable alternatives due to their energy-efficient combined with their high productivity (Flores, Costa, Yamashita, Gerschenson, & Grossmann Eiras, 2010; Pellissari et al., 2012; Thunwall, Boldizar, & Rigdahl, 2006). Particularly, thermo-compression is useful as a processing method because of its simplicity and capability of producing films without polymer solubilization. In this context, these biomaterials could have feasible applications to develop economical and ecological materials (Simkovic, 2013).

The goal of this paper was the development of biodegradable films based on thermoplastic native corn starch containing chitosan and chitin by thermo-compression. Furthermore, the influence of chitin and chitosan addition on films properties (microstructure, color, water vapor permeability, mechanical and dynamic mechanical behavior and antimicrobial capacity) was also studied.

2. Materials and methods

2.1. Materials

Native corn starch was provided by Misky, Arcor (Tucumán, Argentina) with an amylose content of 23.9 ± 0.7 g/100 g (López, García, & Zaritzky, 2010). Chitin was isolated in the Laboratorio de Investigaciones Básicas y Aplicadas en Quitina (LIBAQ) from shrimp shells waste (*Pleoticus mülleri*) supplied by Ingeniero White Port (Bahía Blanca, Argentine). Chitin was previously characterized reporting moisture and ash contents of 0.38 and 6.5 g/100 g, respectively and 6.5 g/100 g nitrogen content (Pistonesi, 2001). Chitosan was prepared by heterogeneous alkaline deacetylation of chitin (Zuñiga, Debbaudt, Albertengo, & Rodríguez, 2010). Chitosan presented a molecular weight (MW) of 468,200 Da, ash and moisture contents of 2.3 and 10.4 g/100 g, respectively and 82.5% of deacetylation degree (DD). To obtain homogeneous size samples chitin and chitosan were sieved employing a sieve with 0.25 mm opening sizes. Glycerol (Anedra, Argentine) was used as plasticizer.

2.2. Thermoplastic starch mixtures

Assayed mixtures were composed by thermoplastic corn starch (TPS) with chitosan or chitin. TPS was based on corn starch with 30 g glycerol and 45 g distilled water/100 g starch. Formulations with two different chitosan concentrations (5 and 10 g/100 g starch) were prepared and designed as TPS–chitosan5 and TPS–chitosan10, respectively. On the other hand, a formulation with 10 g chitin/100 g starch was also prepared (TPS–chitin10). Chitosan or chitin was premixed with starch and then, glycerol and distilled water were added. Samples were mixed and conditioned at 25 °C during 24 h. Mixtures were processed in a Brabender Plastograph (Brabender, Germany) at 140 °C and 50 rpm for 15 min. They were removed from the mixing chamber, triturated and stored at 25 °C and 60% relative humidity (RH) for a week to improve their processability. Ambient conditions were reached employing an aqueous glycerol solution (72 g glycerol/100 g solution).

2.3. Films preparation

TPS films were obtained by thermo-compression using a thermostatized hydraulic press. Processing conditions were 140 °C for 6 min, increasing the pressure every 2 min (80, 140 and 180 kg/cm^2). An aluminum frame as mold of 1 mm thickness and a relation of 1.9 g sample per cm^3 were used. Material was cooled under pressure up to approximately 50 °C, then the pressure was released and obtained films were removed from the frames.

2.4. Films characterization

Before characterization, films were conditioned at 25 °C and 60% RH for a week. Films thickness was measured at different locations of the specimens, employing a micrometer. Ten measurements were taken on each film and mean values are reported.

2.4.1. Fourier transform infrared (FTIR)

FTIR spectra were obtained using a Thermo Nicolet Nexus spectrophotometer (Nicolet, United States). Samples were prepared by mixing TPS films as fine powder with KBr (Sigma Aldrich) at 3 g/100 g. The mixture was pressed and a transparent sample was obtained. Spectra were achieved from 100 accumulated scans at 4 cm^{-1} resolution in the range 4000–400 cm^{-1}.

2.4.2. X-ray diffraction (XRD)

Crystal structure identification of films was studied by XRD. Diffractograms were obtained in an X-ray diffractometer Philips PW1710 (Philips, Holland) with a detector operating at 45 kV and 30 mA within 2Θ varied from 3 to 60°. Crystallinity degree (CD) was calculated as the ratio between the absorption peaks and the total diffractogram area, expressed as percentage (%).

2.4.3. Differential scanning calorimetry (DSC)

Thermal properties of TPS films were determined by DSC in a Perkin Elmer Pyris I (USA) calorimeter. Approximately 10 mg of film were weighted in hermetic pans in order to avoid water loss. An empty hermetic pan was used as reference. Samples were heated from 20 to 250 °C at 10 °C/min, under nitrogen atmosphere. From the thermograms, the following parameters were obtained: onset and melting temperature and melting enthalpy.

2.4.4. Scanning electronic microscopy (SEM)

Homogeneity and appearance of the films were examined by visual observation and by SEM with a JEOL JSM-35 CF electron microscope (JEOL, Japan) using an accelerating voltage of 10 kV. Samples were cryofractured by immersion in liquid nitrogen. Film pieces were mounted on bronze stubs and coated with a gold layer (~30 Å) using an argon plasma metallizer (sputter coater PELCO 91000).

2.4.5. Optical properties

Opacity and UV barrier capacity of films were determined spectrophotometrically. The absorbance spectrum (200–700 nm) was recorded using a Shimadzu UV-160 (Japan) spectrophotometer. Films were cut into rectangles (3 × 1 cm) and placed on the internal side of a quartz spectrophotometer cell. Film opacity (AU nm) was defined as the area under the recorded curve determined by an integration procedure according to Piermaría et al. (2011) and the standard test method for haze and luminous transmittance of transparent plastics recommendations (ASTM D1003-00).

Films color measurements were performed using a Hunterlab UltraScan XE (Hunterlab, USA) colorimeter in the reflectance mode. Color parameters L, a and b were recorded according to the Hunter scale, in at least ten randomly selected positions for each film sample. Color parameters range from $L = 0$ (black) to $L = 100$ (white), $-a$ (greenness) to $+a$ (redness) and $-b$ (blueness) to $+b$ (yellowness). Standard values considered were those of the white background ($L = 97.75$, $a = -0.49$, and $b = 1.96$).

2.4.6. Water vapor permeability (WVP)

WVP was assessed using the ASTM method E96 with several modifications. Samples were sealed over a circular opening of 0.003848 m^2 in a permeation cell that were stored at 25 °C in a permeation camera. The driving force, expressed as water vapor partial pressure, was 1584 Pa. To maintain this driving force corresponding to a 50% relative humidity (RH) gradient across the film, distilled water (100% RH) was placed inside the cell and 50% RH was set in the permeation camera. After steady state conditions were reached, eight weight measurements were made. Samples were analyzed at least by duplicate.

2.4.7. Mechanical properties

Mechanical behavior was measured in an Instron 3369 universal machine (Instron, USA) through tensile tests. For stress-strain tests, ten probes of 13 × 100 mm of each film formulation were assayed. Maximum tensile strength (σ_{max}); elongation at break (Θ_b) and elastic modulus (E) were calculated according to the ASTM D882-00 (1996).

2.4.8. Dynamic mechanical analysis (DMA)

Temperatures and intensities of relaxation phenomena were determined by DMA. Assays were carried out in a dynamic-mechanical thermal equipment Q800 (TA Instruments, New Castle, USA) with a liquid nitrogen cooling system, using a clamp tension. Multi-frequency sweeps (1, 3, 5, 10, 15 and 20 Hz) were carried out at fixed amplitude from −100 to 100 °C at 2 °C/min. Storage (E') and loss (E'') moduli and tan δ curves as a function of temperature were recorded and analyzed using the software Universal Analysis 2000.

2.5. Antimicrobial capacity

Antimicrobial activity was tested against *Escherichia coli* ATCC 25922, *Staphylococcus aureus* ATCC 27933, *Aspergillus* spp. and *Penicillium* spp. Assays were conducted in aseptic conditions, in a laminar flow cabinet (LFC) previously radiated with ultraviolet light for 20 min.

2.5.1. Inocula preparation

Bacteria inoculum: overnight liquid bacteria cultures were diluted in physiological water in the range of 10^5–10^6 CFU mL^{-1}, previously standardized using the McFarland scale.

Fungi inoculum: fungus samples were introduced into test tubes with inclined Potato Dextrose Agar (PDA, Merck, Darmsdat, Germany) and incubated for 5 days at 37 °C. Sterile physiological water (10 mL) was added and stirred over 5 min. Spores were harvested and diluted within the range of 10^5–10^6 CFU mL^{-1} using physiological water standardized by McFarland scale.

2.5.2. Antimicrobial assays

The disk inhibition zone assay was used to qualitatively evaluate the antimicrobial capacity of the films according to Rojas-Graü et al. (2006) with modifications. Films were aseptically cut in 15 mm discs and placed on plates containing Mueller Hinton agar (MHA, Merck, Darmsdat, Germany) for bacteria and PDA for fungi. The plates were previously spread with 0.1 mL of inocula and then incubated at 37 °C for 24 h for bacteria and during 5 days for fungi. Growth inhibition zones around the discs (inhibition halos) and growth under the film discs (area of contact with the agar surface) was visually examined. Tests were carried out in triplicate for each formulation.

2.6. Statistical analysis

A completely randomized experimental design was used to characterize the developed films. Analysis of variance (ANOVA) was used to compare mean differences of the samples characteristics. Besides, comparison of mean values was performed by Fisher's least significant difference test conducted at a significance level $p = 0.05$.

3. Results and discussion

In order to evaluate the influence of chitosan/chitin addition to TPS formulations, films by thermo-compression were obtained. All developed films were homogeneous and easy to handle, with good appearance and constant thickness which varied between 149 and 158 μm.

3.1. FTIR analysis

FTIR analysis was performed in order to study chitosan/chitin addition effects on TPS matrix structure due to interactions between starch, chitosan/chitin and glycerol. Yin, Yao, Cheng, and Ma (1999) stressed that when two or more substances are mixed, physical blends versus chemical interactions are reflected by changes in characteristic spectral bands. Fig. 1 shows FTIR spectra corresponding to TPS matrix, chitosan, chitin, as well as, films based on TPS with chitosan/chitin. TPS spectrum presented bands corresponding to the distinctive functional groups of starch and glycerol. Bands at 920, 985, 1026, 1074 and 1148 cm^{-1} (C–O stretching), 1648 cm^{-1} (bound water), 2929 cm^{-1} (C–H stretching), 3426 cm^{-1} (–OH groups) and 1457 cm^{-1} (glycerol) were observed. Similar results were reported by Zhang and Han (2006). Besides, several bands at low wavenumbers (627, 581, 560 and 400 cm^{-1}) were observed, they were attributed to the skeletal mode vibrations of glucose rings (Kizil, Irudayaraj, & Seetharaman, 2002). Chitosan spectrum showed an absorption band at 3450 cm^{-1-1}, corresponding to stretching of O–H and N–H bonds and several bands at 1031–1156 cm^{-1}, attributed to C–O stretching (Pranoto, Rakshit, & Salokhe, 2005). Moreover, other bands were detected at 2882 cm^{-1} (C–H stretching), at 1594–1663 cm^{-1} (amine groups) and at 1410 cm^{-1} (carboxyl groups). Despite spectra of TPS–chitosan films showed a similar pattern on their informative bands to TPS control film, some modifications were observed (Fig. 1A). The corresponding band located at 3426 cm^{-1} shifted to 3387 and 3329 cm^{-1} for TPS–chitosan5 and TPS–chitosan10, respectively. These changes could be attributed to the interactions by hydrogen bonding between hydroxyl groups of corn starch and amino groups of chitosan. Similar results were reported by Zhong and Xia (2008)

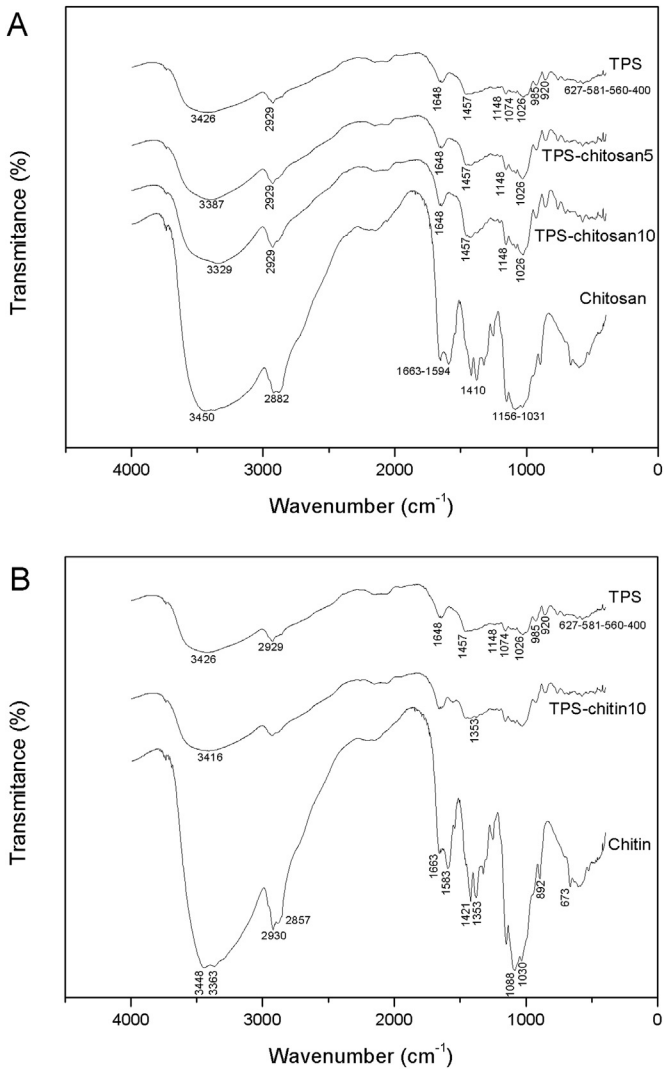

Fig. 1. FTIR spectra of films based on: **A)** thermoplastic corn starch (TPS), chitosan, and TPS with 5 and 10 g chitosan/100 g starch (TPS–chitosan5 and TPS–chitosan10) and **B)** TPS, chitin and TPS with 10 g chitin/100 g starch (TPS–chitin10).

for chitosan and cassava starch mixtures. Intensity of bands at 2929, 1026, 1148, 1648 and 1457 cm^{-1} was increased with chitosan addition due to the increment of the concentration of some functional groups constituents of both biopolymers (starch and chitosan). Particularly, band at 2929 cm^{-1} became more intensive and sharp due to an increase of C–H bonds. Bands at 1648 and 1457 cm^{-1} were more intense for TPS–chitosan10 due to the presence of amine and carboxyl groups, respectively.

Spectrum of chitin (Fig. 1B) was typical of this polysaccharide with very sharper absorption bands due to high crystallinity of this biopolymer (Rinaudo, 2006). Two wide bands at 3363 and 3448 cm^{-1} were detected corresponding to the stretching of O–H and N–H, respectively. The band at 2930 cm^{-1} was attributed to the CH_3 and CH_2 stretching and the one located to 2857 cm^{-1} to CH bonds. The presence of amide I and II groups were evidenced by bands at 1663 and 1583 cm^{-1}, respectively. Besides, other bands were identified at 1421 cm^{-1} (CH_3 deformation and CH_2 bending), 1088 and 892 cm^{-1} (ring stretching), 1030 cm^{-1} (CO) and 673 cm^{-1} (OH bending). All detected bands were in agreement with those reported by Palpandi, Shanmugam, and Shanmugam (2009) for α-chitin (shrimp origin). Spectrum of TPS–chitin10 presented the characteristics bands of TPS, as well as, a less intense band located at 1353 cm^{-1} indicative of acetyl groups of chitin structure (Fig. 1B). As it was described for TPS–chitosan films, a shift of the band located at 3426 cm^{-1} due to the formation of hydrogen bonding between hydroxyl groups of starch and amino groups of chitin, was observed.

Thus, FTIR results revealed changes in TPS matrix due to chitosan/chitin addition attributed mainly to chemical interaction between starch and chitosan/chitin molecules by hydrogen bonding formation.

3.2. X-ray diffraction (XRD)

Quantitative information about TPS crystallinity changes induced by chitosan and chitin presence was obtained by XRD. Patterns for TPS control films, as well as, TPS–chitosan/chitin films are shown in Fig. 2. TPS spectrum presented broad diffraction peaks and a large amorphous scattering background, characteristics of a semi-crystalline polymer with low crystallinity degree. The main reflection peaks which contributed to TPS crystallinity can be detected at 12.8° and 19.6° (Fig. 2). Shi et al. (2006) reported the presence of two sharp peaks located at 13.5° and 20.9° for thermoplastic corn starch with glycerol and they assigned them to V-type structure. This crystalline structure is formed by the crystallization of amylose in single helices involving glycerol or lipids and it can be divided into two subtypes, namely V_a (anhydrous) with peaks at 13.2° and 20.6° and V_h (hydrated) with peaks at 12.6° and 19.4° (Corradini, de Morais, Demarquette, Agnelli, & Mattoso, 2007). Yang, Yu, and Ma (2006) stressed that V_h-style crystallinity is induced by thermal processing where the strong interaction between hydroxyl groups of starch molecules was substituted by hydrogen bonds formed between plasticizer and starch during thermoplastic processing. Therefore, XRD results correlate well with those of FTIR, where this interaction was evidenced.

On the other hand, clear evidence that native corn starch granules were destructed during processing was the absence of the reflection peaks corresponding to the A-type crystal structure, characteristic of cereal starches (Bader & Göritz, 1994; López et al., 2010). Crystalline structure of TPS films with chitosan and chitin resulted similar to that of TPS matrix. However, the addition of these biopolymers increased slightly the degree of crystallinity of TPS matrix, although the differences were not significant (Fig. 2).

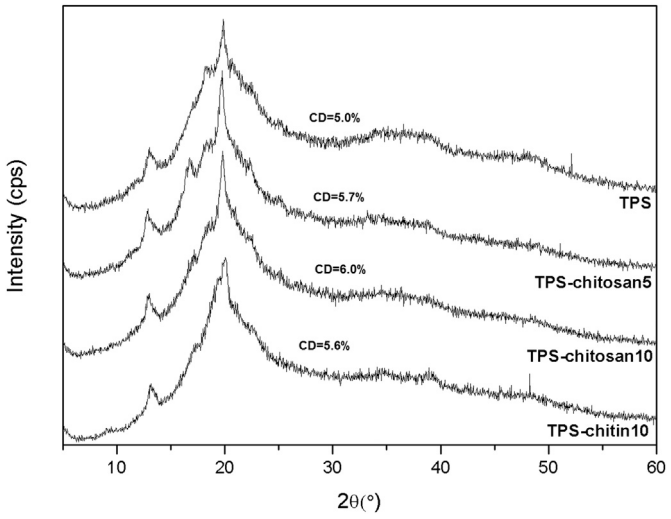

Fig. 2. XRD spectra of films based on thermoplastic corn starch (TPS), TPS with 5 and 10 g chitosan/100 g starch (TPS–chitosan5 and TPS–chitosan10) and TPS with 10 g chitin/100 g starch (TPS–chitin10).

3.3. Differential scanning calorimetry (DSC)

To further understand the structure and interaction between TPS and chitosan/chitin, DSC study of films was performed. Moreover, thermal properties of TPS based materials determine their processing temperature range. All studied TPS films exhibited a single endothermic transition, corresponding to the melting process of the matrix crystalline phase of the as it was shown in Fig. 3. Besides, the occurrence of a single peak is related with the films homogeneity and miscibility among the components. Thermal parameters of the studied films are presented in Table 1. Even though, chitosan and chitin addition to TPS films did not affect significantly ($p > 0.05$) onset and melting temperature, it was registered a slight decrease in their mean values. This shift could be attributed to the interaction between starch and chitosan/chitin molecules, which interrupts the rearrangement of starch polymer chain. This incident can be described in terms of intermolecular forces. In crystalline domains of TPS matrix the interactions between polymeric chains are strong due to their chemical compatibility. When chitosan/chitin was added to TPS formulations crystal lattice was modified, and even though both polymers can interact mainly through hydrogen bonding, interactions between starch chains are weaker, thus less energy is required to disrupt them. When chitosan/chitin was added to TPS formulations crystal lattice was modified, starch molecules are not in optimal positions and their interactions are weaker, thus less energy is required to break them apart. Similarly, Rachtanapun and Wongchaiya (2012) reported that after blending chitosan with methylcellulose the melting point of the obtained film was lower than those corresponding to control ones.

With respect to enthalpy values, a significant decrease with the incorporation of chitosan and chitin was observed, but this effect could not be confirmed by X ray diffraction. Tongdeesoontorn, Mauer, Wongruong, and Rachtanapun (2011) found that a higher interaction between hydrocolloids and starch retained more water molecules, causing a higher mobility during heating, increasing the kinetic energy, and decreasing the enthalpy values.

3.4. Films appearance

SEM was used to evaluate films homogeneity, layer structure, pores and cracks, surface smoothness and thickness. SEM micrographs of fracture surfaces of TPS films are showed in Fig. 4.

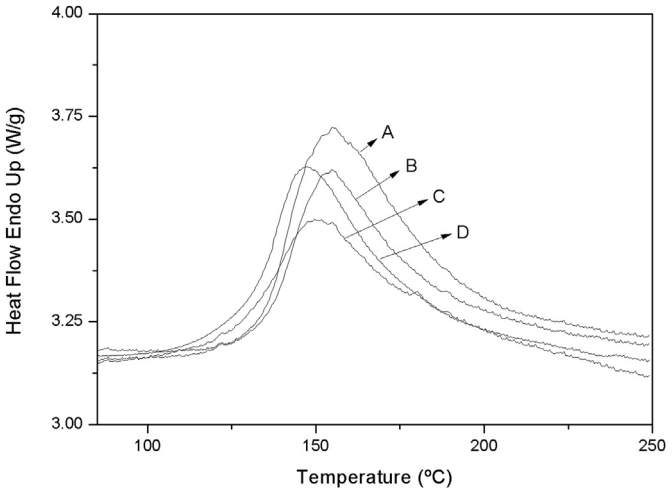

Fig. 3. DSC thermograms of films based on: A) thermoplastic corn starch (TPS), B) TPS with 5 g chitosan/100 g starch, C) and **B)** TPS with 10 g chitosan/100 g starch and D) TPS with 10 g chitin/100 g starch.

Table 1
Thermal properties of films based on thermoplastic corn starch (TPS), TPS with 5 and 10 g chitosan/100 g starch (TPS–chitosan5 and TPS–chitosan10) and TPS with 10 g chitin/100 g starch (TPS–chitin10).

Film formulation	Onset temperature (°C)	Melting temperature (°C)	Melting enthalpy (J/g TPS dry basis)
TPS	137.8 ± 11.0[a]	155.0 ± 12.4[a]	135.2 ± 10.8[a]
TPS–chitosan5	135.4 ± 9.5[a]	154.8 ± 10.8[a]	105.2 ± 7.4[b]
TPS–chitosan10	131.7 ± 11.9[a]	151.7 ± 13.6[a]	89.9 ± 7.5[c]
TPS–chitin10	130.3 ± 10.4[a]	147.2 ± 11.8[a]	94.4 ± 8.5c[d]

Reported values correspond to the mean ± standard deviation. Values within each column followed by different letters indicate significant differences ($p < 0.05$).

TPS control films presented homogeneous and smooth surfaces, without visible pores and cracks. Cross-sections were homogeneous with absence of unmelted starch granules, demonstrating the effectiveness of the destructuration and thermo-compression processes (Fig. 4). These observations are in agreement with X ray diffraction results. Besides, perpendicular channels to film surface which are the evidence of glycerol migration from the matrix were not observed (López, Zaritzky, Grossmann, & García. 2013).

When corn starch was blended with chitosan, film surfaces appeared smooth (without pores and cracks), homogeneous (without phase separation), uniform and flat (Figures not shown). Tomé et al. (2012) reported similar results for TPS–chitosan films obtained by melt-mixing. TPS–chitosan films fractured surface resulted homogeneous, demonstrating that chitosan had not affected starch melting. Cross-section irregularity increased with the increase of chitosan concentration. Although, chitosan was well incorporated to TPS matrix without visible agglomerates observed; irregularities could be attributed to the melt-mixing and thermo-compression methods used. Unlike the reported results by Salleh, Muhamad, and Khairuddin (2009) for films based on starch and chitosan obtained by casting in which chitosan microdomains dispersed within the starch matrix were observed. The compact and homogeneous matrixes of TPS–chitosan films were an indicator of structural integrity, and consequently, good mechanical properties such as high resistance and elongation at break are expected (García, Pinotti, Martino, & Zaritzky, 2009).

TPS–chitin10 films presented homogeneous, smooth, uniform and flat surfaces like TPS–chitosan ones (Figure not shown). However, film cross-sections showed a more irregular structure due to a high rigid phase concentration attributed to chitin moiety.

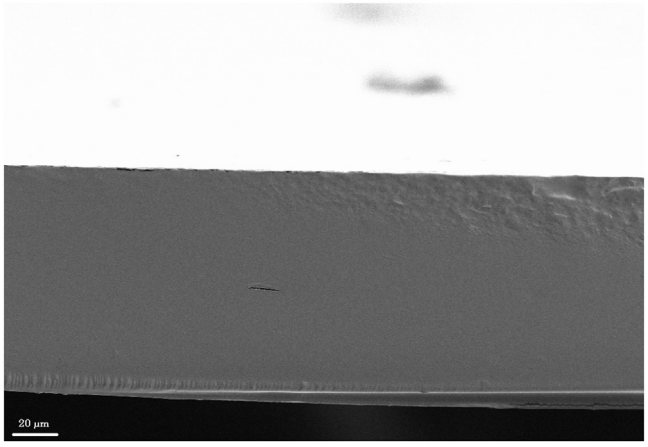

Fig. 4. SEM micrographs (10,000×) of cross-sections of films based on thermoplastic corn starch.

Films thickness was also measured using SEM from cross-section images and values are reported in Table 2. TPS–chitosan/chitin films presented almost constant thickness along the sample and the obtained values were in agreement which those measured with a micrometer. Besides, chitosan and chitin addition to TPS formulations resulted in an increase of films thickness.

3.5. Optical properties

Color attributes are of prime importance because they directly influence consumer acceptability. Color parameters of the developed films are summarized in Table 2. Chitosan addition decreased significantly ($p < 0.05$) the luminosity (L) of TPS films. Parameter a of TPS and TPS–chitosan films were not significantly different ($p > 0.05$). However, parameter b increased significantly ($p < 0.05$) with chitosan concentration. Chillo et al. (2008) developed tapioca starch films with chitosan and glycerol by casting and stressed that L and b parameter increased while a decrease with chitosan addition.

Luminosity values of TPS–chitin10 films was not significantly different ($p > 0.05$) than the corresponding to TPS ones (Table 2). However, chitin addition decreased a parameter while b resulted higher than TPS control films. TPS–chitosan10 films were more yellowish with a b value 77% higher than TPS–chitin10.

Color development in TPS–chitosan/chitin films is related to non enzymatic browning (Maillard reaction). This behavior could mean that processing temperature promoted chemical reactions, such as Maillard reaction, as it was also reported by other authors (Guerrero Beatty, Kerry, & de la Caba, 2012). In the early stage of the Maillard reaction involves the formation of conjugates between the carbonyl group with the amine group in chitosan molecules. This reaction produces a Schiff base, which subsequently cyclizes to produce the Amadori compound and insoluble polymeric compounds, referred as melanoidins, are formed (Leceta, Guerrero, Ibarburu, Dueñas, & de la Caba, 2013; Yasir, Sutton, Newberry, Antrews, & Gerardard, 2007). This reaction is less evident in TPS–chitin films because amino groups in chitin structure are involved in amide bonds and therefore less exposed and susceptible for these reactions.

Fig. 5 corresponds to the UV–vis spectra of the studied films. UV absorption capacity of films allows their application under different conditions in packaging area for a wide range of food, pharmaceutical and cosmetic products. Absorption peak located at 250–300 nm demonstrated that chitosan/chitin added to formulations increased TPS films UV absorption capacity (Table 2). Thus, these films could be useful to extend shelf life of products susceptible to oxidative rancidity.

In Table 2 are also presented film's opacity values. The results obtained indicated that both biopolymers increased opacity values of TPS films. These results are in agreement with those reported by Pelissari et al. (2012) for films based on cassava starch and chitosan.

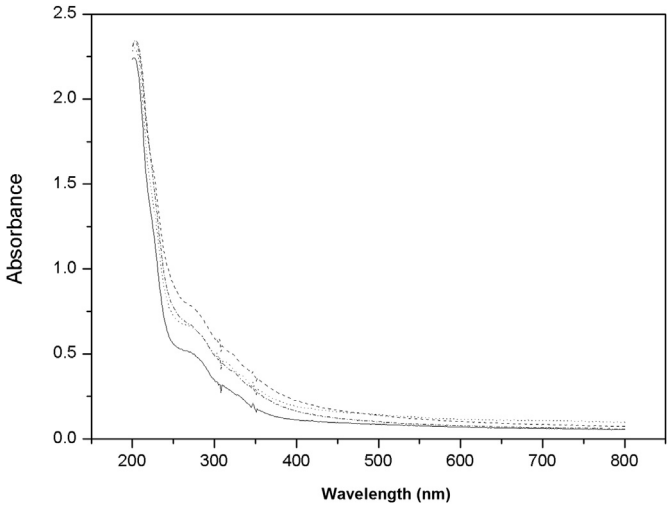

Fig. 5. Absorption spectra (200–700 nm) of films based on thermoplastic corn starch (TPS), TPS with 5 and 10 g chitosan/100 g starch (TPS–chitosan5 and TPS–chitosan10) and TPS with 10 g chitin/100 g starch (TPS–chitin10). TPS (——), TPS–chitosan5 (·····), TPS–chitosan10 (·····) and TPS–chitin10 (-·-·-).

3.6. Water vapor permeability (WVP)

The influence of chitosan/chitin addition on WVP is shown in Table 3, indicating that both biopolymers decreased this barrier property of TPS films. This could be explained by the increase of interactions between chitosan/chitin and corn starch (hydrogen bonding type), which decrease availability of the hydrophilic groups, therefore, the water vapor transmission rate of the matrix decreased (Chillo et al., 2008; Xu et al., 2005). Chemical interaction between starch and chitosan/chitin demonstrated by FTIR reinforced WVP results. Obtained values, as well as, observed tendency were in agreement with those reported by other authors (Chillo et al., 2008; Pelissari et al., 2012). TPS–chitosan films showed lower WVP at higher chitosan concentration. Moreover, WVP values showed that chitin addition had more pronounced effect than chitosan attributed to higher amount of acetyl groups in its structure.

3.7. Mechanical properties

Elastic modulus, maximum tensile strength and elongation at break of TPS–chitosan/chitin films are shown in Table 3. Addition of 10 g chitosan or chitin/100 g starch to TPS matrix increased significantly ($p < 0.05$) films tensile strength. It could be attributed to the intermolecular hydrogen bonding between starch –OH groups with chitosan and chitin $-NH_2$ groups, revealed by FTIR. Similar results were reported by Bourtoom and Chinan (2008) and

Table 2
Thickness, color parameters, opacity and absorption peak area of films based on thermoplastic corn starch (TPS), TPS with 5 and 10 g chitosan/100 g starch (TPS–chitosan5 and TPS–chitosan10) and TPS with 10 g chitin/100 g starch (TPS–chitin10).

Film formulation	Thickness (μm)	Parameter L (luminosity)	Parameter a (green–red)	Parameter b (blue–yellow)	Opacity (AU × nm)	UV absorption peak area (AU × nm)
TPS	110.4 ± 1.6^{a}	92.91 ± 0.20^{a}	-0.21 ± 0.01^{a}	1.16 ± 0.17^{a}	20.0 ± 3.5^{a}	41.9 ± 2.5^{a}
TPS–chitosan5	116.3 ± 2.3^{b}	91.69 ± 0.51^{b}	$-0.24 \pm 0.03^{a,b}$	3.64 ± 0.67^{b}	29.5 ± 0.3^{b}	60.7 ± 3.6^{b}
TPS–chitosan10	137.8 ± 1.5^{c}	90.72 ± 0.40^{c}	$-0.25 \pm 0.04^{a,b}$	5.47 ± 0.73^{c}	37.5 ± 1.0^{c}	74.3 ± 2.3^{c}
TPS–chitin10	121.1 ± 3.1^{b}	$92.47 \pm 1.72^{a,b,c}$	-0.32 ± 0.07^{b}	3.08 ± 1.20^{b}	28.8 ± 0.5^{b}	60.2 ± 2.3^{b}

Reported values correspond to the mean ± standard deviation. Values within each column followed by different letters indicate significant differences ($p < 0.05$).

Table 3
Mechanical properties and water vapor permeability (WVP) of films based on thermoplastic corn starch (TPS), TPS with 5 and 10 g chitosan/100 g starch (TPS–chitosan5 and TPS–chitosan10) and TPS with 10 g chitin/100 g starch (TPS–chitin10).

Film formulation	Elastic modulus (MPa)	Maximum tensile strength (MPa)	Elongation at break (%)	WVP × 10^9 (g/s m Pa)
TPS	1048.6 ± 38.1^{a}	10.7 ± 0.1^{a}	2.36 ± 0.31^{a}	1.33 ± 0.09^{a}
TPS–chitosan5	1136.7 ± 27.4^{b}	$12.4 \pm 1.6^{a,b}$	1.69 ± 0.24^{b}	1.19 ± 0.09^{a}
TPS–chitosan10	1188.4 ± 67.8^{b}	12.5 ± 0.8^{b}	1.64 ± 0.12^{b}	0.87 ± 0.04^{b}
TPS–chitin10	$1080.6 \pm 58.2^{a,b}$	12.6 ± 0.6^{b}	$1.86 \pm 0.44^{a,b}$	0.59 ± 0.02^{c}

Reported values correspond to the mean ± standard deviation. Values within each column followed by different letters indicate significant differences ($p < 0.05$).

Pelissari et al. (2012) studying starch and chitosan films obtained by extrusion.

The elastic modulus indicates the rigidity of the film; a larger value corresponds to a more rigid material (Pelissari et al., 2012). Developed films presented an appreciable rigidity since elastic modulus varied between 1048 and 1188 MPa (Table 3). Elastic modulus increased 8.4 and 13.3% for films containing 5 and 10 g chitosan/100 g starch, respectively. The formation of a dense and rigid matrix could be attributed to their manufacturing process conditions. High temperature, pressure and shear force during melt blending allowed starch chains approximation, which was reinforced with the thermo-compression process. TPS films elastic modulus increase by chitin addition was no significant ($p > 0.05$).

Film's elongation at break is related to flexibility and elongation capacity of the materials. This mechanical parameter was decreased around 30% with the addition of 10 g chitosan/100 g starch to TPS formulations (Table 3). This tendency was reported by several authors and could be related to the TPS matrix crystallinity increase caused by chitosan addition (Bourtoom & Chinan, 2008; Pelissari et al., 2012; Xu et al., 2005). On the other hand, elongation at break reduction observed by chitin addition was not significant ($p > 0.05$).

3.8. Dynamic mechanical analysis (DMA)

Dynamic mechanical properties are related to the structure and morphology of polymeric materials (Tuhin et al., 2012). DMA is a sensitive technique to evaluate glass transitions associated to the phase relaxation behavior of polymeric systems. Multi-frequency assays (1, 3, 5, 10, 15 and 20 Hz) were performed as it was shown in Fig. 6 for TPS–chitosan10 films. Regardless the frequency, similar dynamic mechanical behavior was evidenced for all studied TPS films. DMA relaxation spectra performed at 3 Hz of TPS control film are shown in Fig. 7. Storage modulus (E') is related to the composite stiffness and it is the elastic response whereas loss modulus (E'') is the viscous response of the material. Loss factor is defined as $\tan\delta = E''/E'$ and it is related to the molecular motion. In the case of TPS control films, DMA spectrum presented two thermal transitions due to the presence of two separate phases (Fig. 7). This behavior was mainly evidenced in loss modulus curves. Several authors stressed that the upper transition corresponds to a starch-rich phase whereas the lower one is associated to a glycerol-rich phase (Da Roz, Carvalho, Gandini, & Curvelo, 2006; García et al., 2009; López, Lecot, Zaritzky, & García, 2011; Mathew & Dufresne, 2002). As it is shown in Fig. 7, the transition associated to the starch-rich phase was not completely defined due to the low resistance to softening of TPS films during the assays. In this sense, several authors have reported that plasticizer-rich phase transition for different TPS matrixes has a better definition with a higher intensity change than the second one attributed to the starch-rich

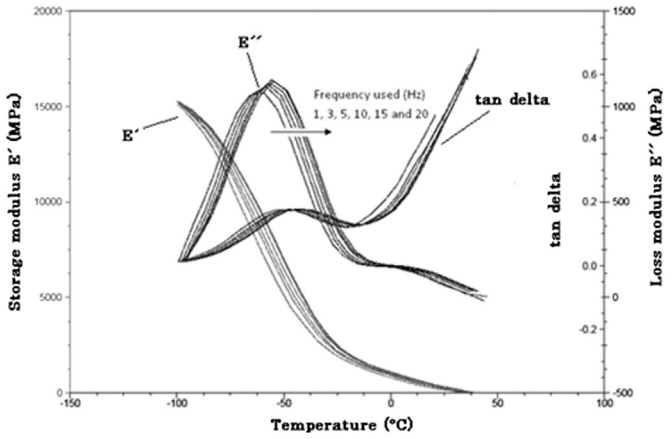

Fig. 6. DMA spectra of films based on thermoplastic corn starch with 10 g chitosan/100 g starch. Dependence of E' (storage modulus), E'' (loss modulus) and tan δ with temperature at a constant frequency of 1, 3, 5,10, 15 and 20 Hz.

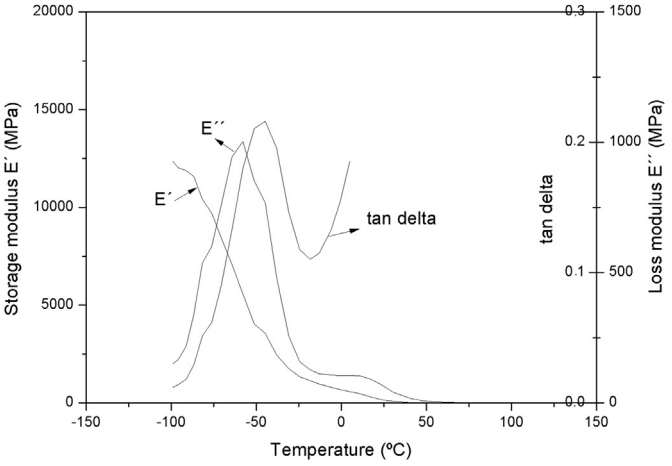

Fig. 7. DMA spectra of films based on thermoplastic corn starch. Dependence of E' (storage modulus), E'' (loss modulus) and tan δ with temperature at a constant frequency of 3 Hz.

phase (Famá, Flores, Gerschenson, & Goyanes, 2006; Forsell, Mikkilä, Moates, & Parker, 1997; Hongsprabhas & Israkarn, 2008; Jiang, Qiao, & Sun, 2006; López et al., 2011; Ma, Chang, Yu, & Stumborg, 2009; Wilhelm, Sierakowski, Souza, & Wypych, 2003). For TPS–chitosan/chitin films, a similar behavior was observed since E'' curves also revealed two separate transitions associated to the presence of distinctive domains enriched in glycerol or in starch

Table 4
Relaxation temperatures associated to the glass transition of the glycerol-rich phase of films based on thermoplastic corn starch (TPS), TPS with 5 and 10 g chitosan/100 g starch (TPS–chitosan5 and TPS–chitosan10) and TPS with 10 g chitin/100 g starch (TPS–chitin10) determined by DMA (3 Hz).

Film formulation	Relaxation temperatures associated to the glass transition of the glycerol-rich phase (°C)		
	Inflexion of storage modulus (E')	Maximum of loss modulus (E'')	Maximum of tan δ
TPS	-68.0 ± 0.6^{a}	-60.5 ± 4.1^{a}	-51.8 ± 1.0^{a}
TPS–chitosan5	-66.9 ± 2.5^{a}	-61.8 ± 4.1^{a}	-52.0 ± 0.9^{a}
TPS–chitosan10	-65.1 ± 4.7^{a}	-55.7 ± 3.8^{a}	-48.9 ± 5.9^{a}
TPS–chitin10	-66.2 ± 3.2^{a}	-56.8 ± 3.1^{a}	-50.4 ± 3.8^{a}

Reported values correspond to the mean ± standard deviation. Values within each column followed by different letters indicate significant differences ($p < 0.05$).

throughout the TPS matrix (Figures not shown). The similitude between DMA spectra may be attributed to the compatibility between starch, chitosan and chitin that makes very difficult separating glass transitions events of individual polymeric constituents in biocomposites. Moreover, obtained results indicated that these biopolymers presented a similar plasticization behavior. Chitosan and chitin addition affected positively storage (E') and loss (E'') moduli, which indicates a better elastic and viscous response of TPS films.

Glass transition temperatures (T_g) were determined through the inflexion point of the E' curve and the maximum in E'' and tan δ curves (Psomiadou, Arvanitoyannis, & Yamamoto, 1996). Knowledge of T_g is important since it impacts on films mechanical and barrier properties under specific conditions of application and storage. Relaxation temperatures associated to glass transition of glycerol-rich phase for all developed TPS films are presented in Table 4. Despite there is no significant differences ($p > 0.05$) among relaxation temperatures corresponding to glycerol-rich phase, an

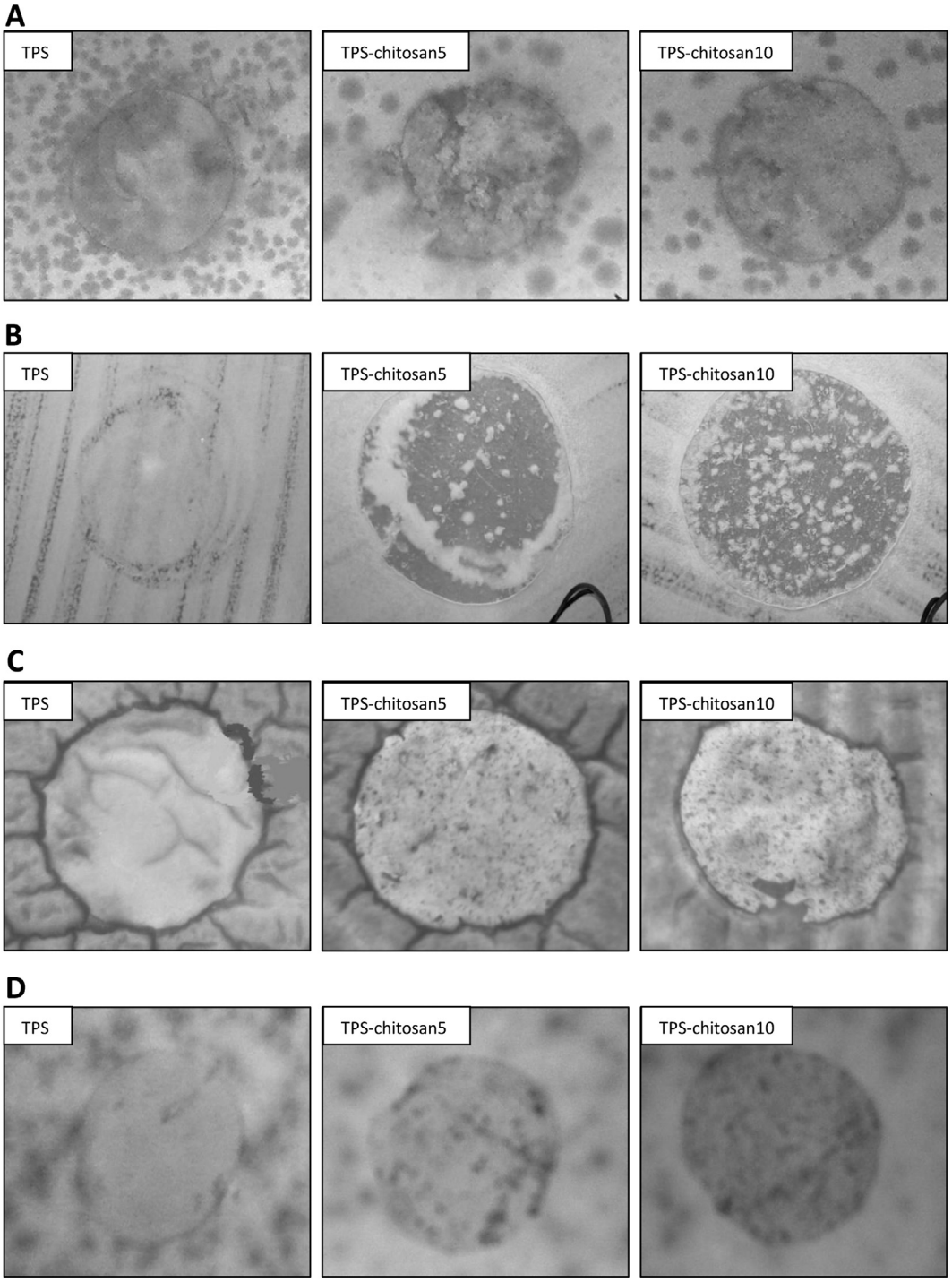

Fig. 8. Antimicrobial capacity of films based on thermoplastic corn starch (TPS) and TPS with 5 and 10 g chitosan/100 g starch (TPS–chitosan5 and TPS–chitosan10) against: **A)** *Staphylococcus aureus* ATCC 27933, **B)** *Escherichia coli* ATCC 25922, **C)** *Aspergillus* spp., and **D)** *Penicillium* spp.

increase in their mean values were observed. The shift of the relaxation temperature to a higher value is indicative of restricted molecular movement (Piyada, Waranyou, & Thawien, 2013). In this particular case, this shift is the consequence of chemical interactions through hydrogen bonding between hydroxyl groups of starch and amino groups of chitosan and chitin, evidenced by FTIR results. Chang, Jian, and Ma (2010) reported that the T_g of glycerol plasticized-potato starch film shifted to higher temperature by chitin nanoparticles addition.

3.9. Antimicrobial capacity

Antimicrobial capacity was tested against two food pathogenic bacteria: *E. coli* and *S. aureus*. Besides, studies against two usual spoilage fungi (*Aspergillus* spp. and *Penicillium* spp.) were also carried out. The studied fungi are known due to its resistant to several stress factors commonly used in food elaboration such as decreasing pH, incorporation of high levels of sugar and pasteurizations. Details of antimicrobial capacity of TPS films containing chitin and chitosan are shown in Fig. 8. As it was expected, despite of the well-known chitosan antimicrobial properties, it was not observed any clear zone surrounding circular film strips for all studied formulations. This result is attributed to the incapacity of this macromolecule to diffuse through the adjacent agar media. Chitosan in a solid form only inhibits organisms in direct contact with the active sites of this biopolymer (Coma et al., 2002; Pranoto et al., 2005). Furthermore, processing method for film preparation led to strong interactions between starch hydroxyl and chitosan amino groups that affected the diffusion phenomenon of chitosan from the TPS matrix.

Visual examination of *S. aureus* growth in the contact area indicated that TPS formulations with the highest chitosan concentration presented highest growth inhibition, with better film integrity than control films (Fig. 8A). Furthermore, it was observed that chitosan presence in TPS films modified *S. aureus* growth, decreasing the number of colonies (Fig. 8A). Antimicrobial activity studies of active films against *E. coli* revealed that chitosan presented an inhibitory effect limiting growth of this microorganism underneath film disks (Fig. 8B). This result was more pronounced for the highest chitosan concentration studied. On the other hand, there was no effect on *Penicillium* spp and *Aspergillus niger* for both inhibitory and contact zones for all chitosan concentrations employed in this research (Fig. 8C and D). This result could be attributed to the used method. Thus, it is relevant to standardize testing conditions for the optimum design of active antimicrobial food packaging films and coating applications. Incorporating chitin into formulations did not modify antimicrobial efficacy of TPS films against all tested microorganisms.

4. Conclusions

Thermo-compression films of thermoplastic corn starch with chitosan/chitin had uniform thickness and good appearance. FTIR results suggested some structural modifications in TPS matrix attributed to the interactions between starch hydroxyl and chitosan/chitin amino groups. DSC studies demonstrated that chitosan and chitin incorporation decreased enthalpy melting values of TPS films. SEM micrographs showed that films presented homogeneous and smooth surfaces, without pores and cracks and no glycerol migration. Thermo-compression effectiveness was demonstrated by homogeneous cross-sections with absence of unmelting starch granules and no visible agglomerates of chitin and chitosan. TPS films luminosity decreased with chitosan content. TPS–chitosan/chitin films presented color development related to non enzymatic browning, as well as, a higher UV absorption capacity and opacity than control ones. WVP was reduced with chitosan/chitin incorporation. Addition of these biopolymers to TPS increased tensile strength and elastic modulus and decreased elongation at break. DMA assays evidenced the presence of two distinctive domains enriched in glycerol or in starch. Antimicrobial capacity demonstrated that TPS films with chitosan reduced *S. aureus* and *E. coli* growth in the contact zone. These results are relevant achievements in relation to the potential production of biodegradable packaging at industrial scale using biopolymers as raw material.

References

American Society for Testing and Materials-ASTM. (1996). *Standard test methods for tensile properties of thin plastic sheeting*. D882-91. Philadelphia, PA: Annual Book of ASTM.

Bader, H., & Göritz, D. (1994). Investigation on high amylose corn starch films. *Starch/Stärke, 48*(3), 94–101.

Bourtoom, T., & Chinan, M. (2008). Preparation and properties of rice starch-chitosan blend biodegradable film. *Food Science and Technology, 41*, 1633–1641.

Carvalho, A., Job, A., Alves, N., Curvelo, A., & Gandini, A. (2003). Thermoplastic starch/natural rubber blends. *Carbohydrate Polymers, 53*, 95–99.

Chang, P., Jian, R., & Ma, X. (2010). Fabrication and characterization of chitosan nanoparticles/plastised-starch composites. *Food Chemistry, 120*, 736–740.

Chillo, S., Flores, S., Mastromatteo, M., Conte, A., Gerschenson, L., & Del Nobile, M. A. (2008). Influence of glycerol and chitosan on tapioca starch-based edible film properties. *Journal of Food Engineering, 88*, 159–168.

Coma, V., Martial-Gros, A., Garreau, S., Copinet, A., Salin, F., & Deschamps, A. (2002). Edible antimicrobial films based on chitosan matrix. *Journal of Food Science, 67*(3), 1162–1169.

Corradini, E., de Morais, L., Demarquette, N., Agnelli, J., & Mattoso, L. (2007). Study of process parameters for starch, gluten, and glycerol mixtures. *Advanced Polymer Technology, 18*, 861–867.

Da Roz, A., Carvalho, A., Gandini, A., & Curvelo, A. (2006). The effects of plasticizers on thermoplastic starch compositions obtained by melt processing. *Carbohydrate Polymers, 63*, 417–424.

Fajardo, P., Martins, J. T., Fuciños, C., Pastrana, L., Teixeira, J. A., & Vicente, A. A. (2010). Evaluation of a chitosan-based edible film as carrier of natamycin to improve the storability of Saloio cheese. *Journal of Food Engineering, 101*, 349–356.

Famá, L., Flores, S., Gerschenson, L., & Goyanes, S. (2006). Physical characterization of cassava starch biofilms with special reference to dynamic mechanical properties at low temperatures. *Carbohydrate Polymers, 66*, 8–15.

Fishman, M., Coffin, D., Konstance, R., & Onwulata, C. (2000). Extrusion of pectin/starch blends plasticized with glycerol. *Carbohydrate Polymers, 41*(4), 317–325.

Flores, S., Costa, D., Yamashita, F., Gerschenson, L., & Grossmann Eiras, M. (2010). Mixture design for evaluation of potassium sorbate and xanthan gum effect on properties of tapioca starch films obtained by extrusion. *Materials Science & Technology, 30*(1), 196–202.

Forssell, P., Mikkilä, J., Moates, G., & Parker, R. (1997). Phases and glass transition behaviour of concentrated barley starch-glycerol-water mixtures, a model for thermoplastic starch. *Carbohydrate Polymers, 34*, 275–282.

García, M., Pinotti, A., Martino, M., & Zaritzky, N. (2009). Characterization of starch and composite edible films and coatings. In M. Embuscado, & K. Huber (Eds.), *Edible films and coatings for food applications* (pp. 169–209). New York: Springer.

Guerrero, P., Beatty, E., Kerry, J. P., & de la Caba, K. (2012). Extrusion of soy protein with gelatin and sugars with at low moisture content. *Journal of Food Engineering, 110*(1), 53–59.

Hongsprabhas, P., & Israkarn, K. (2008). New insights on the characteristics of starch network. *Food Research International, 41*, 998–1006.

Jiang, W., Qiao, X., & Sun, K. (2006). Mechanical and thermal properties of thermoplastic acetylated starch/poly(ethylene-co-vinyl alcohol) blends. *Carbohydrate Polymers, 65*, 139–143.

Kizil, R., Irudayaraj, J., & Seetharaman, K. J. (2002). Characterization of irradiated-starches by using FT-Raman and FTIR spectroscopy. *Journal of Agricultural and Food Chemistry, 50*, 3912–3918.

Lazaridou, A., & Biliaderis, C. (2002). Thermophysical properties of chitosan. Chitosan-starch and chitosan-pullulan films near the glass transition. *Carbohydrate Polymers, 48*, 179–190.

Leceta, I., Guerrero, P., Ibarburu, I., Dueñas, M. T., & de la Caba, K. (2013). Characterization and antimicrobial analysis of chitosan-based films. *Journal of Food Engineering, 116*, 889–899.

Le, X. T., Nagasawa, N., Matsuhashi, S., Ishioka, N. S., Ito, T., & Kume, T. (2001). Effect of radiation-degraded chitosan on plants stressed with vanadium. *Radiation Physics and Chemistry, 61*, 171–175.

Liu, X. F., Huang, Y. L., Yang, D. Z., Li, Z., & Yao, K. D. (2001). Antibacterial action of chitosan and carboxymethylated chitosan. *Journal of Applied Polymer Science, 79*, 1324–1335.

López, O., García, M., & Zaritzky, N. (2010). Physicochemical characterization of chemically modified corn starches related to rheological behavior, retrogradation and film forming capacity. *Journal of Food Engineering, 100*(1), 160–168.

López, O., Lecot, C., Zaritzky, N., & García, M. (2011). Biodegradable packages development from starch based heat sealable films. *Journal of Food Engineering, 105*(2), 254–263.
López, O., Zaritzky, N., Grossmann, M. V. E., & García, M. (2013). Acetylated and native corn starch blend films produced by blown extrusion. *Journal of Food Engineering, 116*(2), 286–297.
Ma, X., Chang, P., Yu, J., & Stumborg, M. (2009). Properties of biodegradable citric acid-modified granular starch/thermoplastic pea starch composites. *Carbohydrate Polymers, 75*, 1–8.
Mali, S., Karam, L. B., Pereira Ramos, L., & Grossmann, M. V. E. (2004). Relationships among the composition and physicochemical properties of starches with the characteristics of their films. *Journal of Agricultural and Food Chemistry, 52*, 7720–7725.
Martin, O., Schwach, E., Avérous, L., & Couturier, Y. (2001). Properties of biodegradable multilayer films based on plasticized wheat starch. *Starch/Stärke, 53*, 372–380.
Mathew, A., & Dufresne, A. (2002). Morphological investigation of nanocomposites from sorbitol plasticized starch and tunicin whiskers. *Biomacromolecules, 3*, 609–617.
Palpandi, C., Shanmugam, V., & Shanmugam, A. (2009). Extraction of chitin and chitosan from shell and operculum of mangrove gastropod *Nerita (Dostia) crepidularia* Lamarck. *International Journal of Medicine and Medical Science, 1*(5), 198–205.
Pelissari, F. M., Yamashita, F., García, M. A., Martino, M. N., Zaritzky, N. E., & Grossmann, M. V. E. (2012). Constrained mixture design applied to the development of cassava starch-chitosan blown films. *Journal of Food Engineering, 108*, 262–267.
Pelissari, F. M., Yamashita, F., & Grossmann, M. V. E. (2011). Extrusion parameters related to starch/chitosan active films properties. *International Journal of Food Science and Technology, 46*, 702–710.
Piermaria, J., Bosch, A., Pinotti, A., Yantorno, O., Garcia, M. A., & Abraham, A. G. (2011). Kefiran films plasticized with sugars and polyols: water vapor barrier and mechanical properties in relation to their microstructure analyzed by ATR/FT-IR spectroscopy. *Food Hydrocolloids, 25*(5), 1261–2126.
Pistonesi, M. (2001). *Obtención de quitosano estándar y su aplicación para el tratamiento de aguas y efluentes industriales*. Tesis doctoral. Argentina: Universidad Nacional del Sur.
Piyada, K., Waranyou, S., & Thawien, W. (2013). Mechanical, thermal and structural properties of rice starch films reinforced with rice starch nanocrystals. *International Food Research Journal, 20*(1), 439–449.
Pranoto, Y., Rakshit, S. H., & Salokhe, V. M. (2005). Enhancing antimicrobial activity of chitosan films by incorporating garlic oil, potassium sorbate and nisin. *LWT – Food Science and Technology, 38*(8), 859–865.
Psomiadou, E., Arvanitoyannis, I., & Yamamoto, N. (1996). Edible films made from natural resources; microcrystalline cellulose (MCC), methylcellulose (MC) and corn starch and polyols: part 2. *Carbohydrate Polymers, 31*, 194–204.
Quattara, B., Simard, R. E., Piette, G., Begin, A., & Holley, R. A. (2000). Diffusion of acetic and propionic acids from chitosan-based antimicrobial packaging films. *Journal of Food Science, 65*(5), 768–773.
Rachtanapun, P., & Wongchaiya, P. (2012). Effect of relative humidity on mechanical properties of blended chitosan-methylcellulose film. *Chiang Mai Journal of Science, 39*(1), 133–137.
Rinaudo, M. (2006). Chitin and chitosan: properties and applications. *Progress in Polymer Science, 31*, 603–632.
Rojas-Graü, M. A., Avena-Bustillos, R. J., Friedman, M., Henika, P. R., Martin-Bellosos, O., & McHugh, T. H. (2006). Mechanical barrier and antimicrobial properties of apple puree edible films containing plant essential oils. *Journal of Agricultural and Food Chemistry, 54*, 9262–9267.
Salleh, E., Muhamad, I., & Khairuddin, N. (2009). Structural characterization and physical properties of antimicrobial (AM) starch-based films. *World Academy of Science, Engineering and Technology, 31*, 428–436.
Shi, R., Liu, Q., Ding, T., Han, Y., Zhang, L., Chen, D., et al. (2006). Ageing ofsoft thermoplastic starch with high glycerol content. *Journal of Applied Polymer-Science, 103*, 574–586.
Simkovic, I. (2013). Unexplored possibilities of all-polysaccharide composites. *Carbohydrate Polymers, 95*, 697–715.
Sothornvit, R., Olsen, C. W., McHugh, T. H., & Krochta, J. M. (2007). Tensile properties of compression-molded whey protein sheets: determination of molding condition and glycerol-content effects and comparison with solution-cast films. *Journal of Food Engineering, 78*, 855–860.
Thunwall, M., Boldizar, A., & Rigdahl, M. (2006). Compression molding and tensile properties of thermoplastic potato starch materials. *Biomacromolecules, 7*, 981–986.
Thunwall, M., Kuthanova, V., Boldizar, A., & Rigdahl, M. (2008). Film blowing of thermoplastic starch. *Carbohydrate Polymers, 71*, 583–590.
Tomé, L. C., Fernandes, S. C. M., Sadocco, P., Causio, J., Silvestre, A. J. D., Neto, C. P., et al. (2012). Antibacterial thermoplastic starch-chitosan based materials prepared by melt mixing. *BioResources, 7*(3), 3398–3409.
Tongdeesoontorn, W., Mauer, L. J., Wongruong, S., & Rachtanapun, P. (2011). Effect of carboxymethyl cellulose concentration on physical properties of biodegradable cassava starch-based films. *Chemistry Central Journal, 5*(1), 6–13.
Tuhin, M. O., Rahman, N., Haque, M. E., Khan, R. A., Dafader, N. C., Islam, R., et al. (2012). Modification of mechanical and thermal property of chitosan–starch blend films. *Radiation Physics and Chemistry, 81*, 1659–1668.
Wilhelm, H., Sierakowski, M., Souza, G., & Wypych, F. (2003). Starch films reinforced with mineral clay. *Carbohydrate Polymers, 52*, 101–110.
Xu, Y. X., Kimb, K. M., Hanna, M. A., & Nag, D. (2005). Chitosan–starch composite film: preparation and characterization. *Industrial Crops and Products, 21*(2), 185–192.
Yang, J., Yu, J., & Ma, X. (2006). Study on the properties of ethylene bis formamide and sorbitol plasticized corn starch (ESPTPS). *Carbohydrate Polymers, 66*(1), 110–116.
Yasir, B. M., Sutton, K. H., Newberry, M. P., Antrews, N. R., & Gerardard, J. A. (2007). The impact of Maillard crosslinking on soy proteins ad tofu texture. *Food Chemistry, 104*(4), 1502–1508.
Yin, Y. L., Yao, K. D., Cheng, G. X., & Ma, J. B. (1999). Properties of polyelectrolyte complex films of chitosan and gelatin. *Polymer International, 48*, 429–433.
Zhai, M., Zhao, L., Yoshii, F., & Kume, T. (2004). Study on antibacterial starch/chitosan blend film formed under the action of irradiation. *Carbohydrate Polymers, 55*(1), 83–88.
Zhang, Y., & Han, J. (2006). Mechanical and thermal characteristics of pea starch films plasticized with monosaccharides and polyols. *Journal of Food Science, 71*, 109–111.
Zhong, Q. P., & Xia, W. S. (2008). Physicochemical properties of chitosan-based films. *Food Technology and Biotechnology, 46*(3), 262–269.
Zuñiga, A., Debbaut, A., Albertengo, L., & Rodríguez, M. S. (2010). Synthesis and characterization of N-propyl-N-methylene phosphonic chitosan derivative. *Carbohydrate Polymers, 79*, 475–480.